EurJOC European Journal of Organic Chemistry

FULL PAPER

DOI: 10.1002/ejoc.201500599

Ureido-Pyridazinone Derivatives: Insights into the Structural and Conformational Properties for STAT3 Inhibition

Fiorella Meneghetti,[a] Stefania Villa,*[a] Daniela Masciocchi,[a] Daniela Barlocco,[a] Lucio Toma,[b] Dong-Cho Han,[c] Byoung-Mog Kwon,[c] Naohisa Ogo,[d] Akira Asai,[d] Laura Legnani,*[b] and Arianna Gelain[a]

Keywords: Medicinal chemistry / Cancer / Inhibitors / Signal transduction / Conformation analysis / Proteins

Three new ureido-pyridazinone derivatives, which are structurally related to the known STAT3 inhibitor **AVS-0288**, were designed by taking into account the structure–activity relationships determined for several ureido-oxadiazole derivatives previously studied by our group. Their synthesis was first attempted through suitable 5-aminopyridazinone intermediates (**6a** and **6b**), which molecular structures were confirmed by means of X-ray diffraction data on **6a**. Amine functionalization was unsuccessful, therefore, an alternative method was devised. Dual-luciferase and AlphaScreen-based assays were used to test their activity. The obtained data were rationalized on the basis of a modeling study, which focused our attention on the geometrical preferences of the ureido moiety. Computational results seem to indicate that both the 1,2,5-oxadiazole ring and the extended *ZZ* arrangement are essential and probably act in a synergistic way to confer significant activity against STAT3.

Introduction

Signal transducer and activator of transcription 3 (STAT3) is a member of a STAT family that is made up of seven isoforms (STAT1-4, 5a, 5b, 6).[1] They directly relay signals from the cytoplasmic membrane to the nucleus and regulate transcription of target genes.[2] STATs have several retained domains of which the Src Homology 2 (SH2) domain is fundamental for STATs activation, which is regulated by phosphorylation of a specific tyrosine residue (Tyr705) by kinases. Phosphorylated STAT3 proteins form homodimers and/or heterodimers with STAT1 through reciprocal phosphotyrosine-SH2 interaction. The active dimers translocate into the nucleus where they bind to consensus-promoter sequences of target genes[2] and modulate their transcription. STAT3 is constitutively activated in a wide variety of human solid and blood tumors.[3] Numerous published reports have shown that a block on activated STAT3 signaling leads to apoptosis of tumors cells[4,5] with minimal effect on normal cells.[6–8] Therefore, STAT3 has been proven to be a valid molecular target for cancer therapy.

In the recent years, ureido-oxadiazole derivative **AVS-0288 (I)**[9] was disclosed as a potent inhibitor of the STAT3 pathway (Figure 1), in a STAT3-dependant luciferase reporter assay.

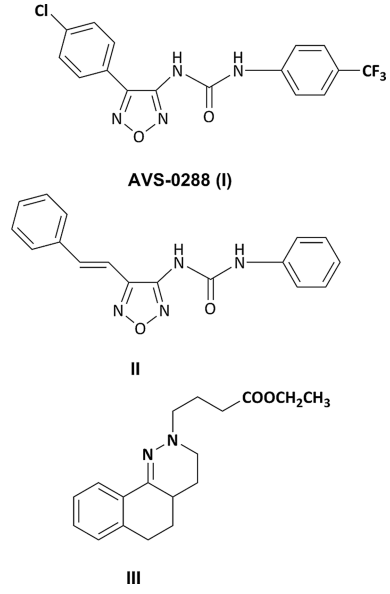

Figure 1. Chemical structures of the reference compounds.

[a] Dipartimento di Scienze Farmaceutiche, Università degli Studi di Milano,
Via L. Mangiagalli 25, 20133 Milano, Italy
E-mail: stefania.villa@unimi.it
http://www.disfarm.unimi.it
[b] Dipartimento di Chimica, Università degli Studi di Pavia,
Via Taramelli 12, 27100 Pavia, Italy
[c] Laboratory of Chemical Biology and Genomics, Korea Research Institute of Bioscience & Biotechnology and Department of Biomolecular Science, University of Science and Technology,
Eoun-Dong, Yuseong-gu, Daejeon 305-333, South Korea
[d] Center for Drug Discovery, Graduate School of Pharmaceutical Sciences, University of Shizuoka,
52-1 Yada, Suruga-ku, Shizuoka, 422-8526, Japan

Supporting information for this article is available on the WWW under http://dx.doi.org/10.1002/ejoc.201500599.

Recently, we performed a modeling study on **I** to understand its conformational preferences.[10] Computational data revealed, in the gas phase, complete preference of **I** for a bent *EZ* arrangement around the two amide bonds, favored by formation of an intramolecular H-bond between an ureido NH hydrogen and the oxadiazole N2 atom. However, the solvent deeply influences the conformational preferences of **I**. In water, the extended *ZZ* arrangement is largely preferred. ^{1}H NMR spectroscopic studies in solvents with different polarity confirmed the modeling results. In addition, an X-ray diffraction study showed for **I** a molecular feature that corresponds to the *ZZ* arrangement calculated in water.

Amongst many other compounds structurally related to **I**, synthesized by us as possible STAT3 inhibitors, styryl derivative **II** (Figure 1), for which the bent *EZ* arrangement of the urea group was shown both in the solid state[11] and by theoretical calculations in vacuo and in water (unpublished results), showed a significant drop in activity with respect to **I**.[11] The computational results show, both in vacuo (100%) and in water (>99%), complete preference for the *EZ* arrangement at the ureido moiety and the formation of an intramolecular H-bond between an ureido NH hydrogen and the oxadiazole N2 atom.

These results prompted us to assume that the extended *ZZ* arrangement of the ureido moiety was a key geometrical feature for STAT3 inhibition. On this basis, we have now synthesized compounds **1** and **2** by replacing the 1,2,5-oxadiazole with the pyridazinone ring and linking the ureido group at position 5 of the heterocycle, to prevent formation of the intramolecular hydrogen bond. We took advantage of our experience in the chemistry of pyridazinone systems, which was exploited in previous studies, in which this nucleus was inserted in several benzocinnolinone derivatives such as compound **III** (Figure 1) that showed the most promising activity.[12]

This paper describes the synthesis, conformational, and biological properties of compounds **1** and **2** (Figure 2).

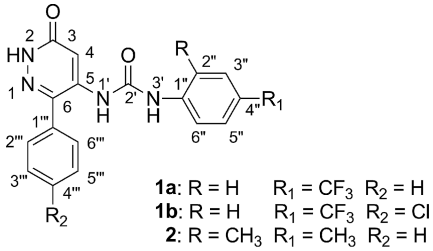

Figure 2. General structure of the title compounds.

Results and Discussion

Chemistry

Two different synthetic procedures were attempted for compounds **1**. In the first approach (see Supporting Information) by following a procedure previously described for **6a**[13], analogue **6b** was obtained from chlorobenzene by condensation with mucochloric acid to give **3b**, which was subsequently cyclized with hydrazine to give **4b**. Replacement of the aryl chlorine with sodium azide led to **5b**, which was hydrogenated to give key intermediate **6b** in the presence of Pd/$BaSO_4$ to avoid loss of the chlorine atom. However, **6a** and **6b** did not react with 4-(trifluoromethyl)phenyl isocyanate under various experimental conditions, although single-crystal X-ray analysis on **6a** unambiguously supported their structure (see Supporting Information). The reactivity of both **6a** and **6b** was tested through treatment with acetic anhydride at reflux temperatures, but the expected[13] acetylated products were not obtained.

Therefore, an alternative synthetic pathway was designed that successfully led to desired pyridazinones **1** and **2** (Scheme 1). Following a procedure already described for the preparation of **13a**,[14] analogue **13b** was prepared from commercially available 4-chlorobenzoyl propionic acid through a hydroxymethylation reaction with formaldehyde and sodium hydroxide in water, and subsequent cyclization in acidic conditions to give intermediate **7b**.[15] Treatment of the intermediate with a large excess of hydrazine monohydrate gave compound **8b**, which was protected on the alcoholic function by acetic anhydride (**9b**) and then dehydrogenated with activated manganese dioxide to give aromatic derivative **10b**. Removal of the protecting group (see **11b**), followed by oxidation with activated manganese dioxide led to corresponding aldehydic intermediate **12b**, which underwent further oxidation to carboxylic acid **13b** by treatment with silver oxide.

Both carboxylic acids **13a** and **13b** by means of a Curtius rearrangement with diphenyl phosphoryl azide in toluene led to isocyanate derivatives, which were not isolated but were directly converted into final ureidic products **1a** and **1b** by coupling with 4-(trifluoromethyl)aniline. Similarly, **13a** was converted into ureidic product **2** by coupling with 2,4-dimethylphenyl aniline.

Modeling Studies

To determine the effects of replacement of the oxadiazole with pyridazinone on the conformational properties of the synthesized compounds, an in-depth modeling study of **1a** was performed. All its degrees of conformational freedom were considered, with particular attention to: (i) the relative orientation of the ureido chain with respect to the pyridazinone ring (τ_1: C4–C5–N1′–C2′); (ii) the different arrangements of the ureido moiety (τ_2: C5–N1′–C2′–N3′; τ_3: N1′–C2′–N3′–C1′′); and (iii) the relative orientation of the ureido chain with respect to the phenyl ring (τ_4: C2′–N3′–C1′′–C2′′). After optimization of the various starting geometries at the B3LYP level with the 6-311+G(d,p) basis set,[16] the located conformers were grouped, on the basis of the values of τ_1, into two families, A and B, characterized by having, respectively, the N1′ hydrogen atoms pointing towards the aryl group or in the opposite direction. Within each family, the members differ for the arrangements of the ureido moiety. In fact, depending on the dihedral angle val-

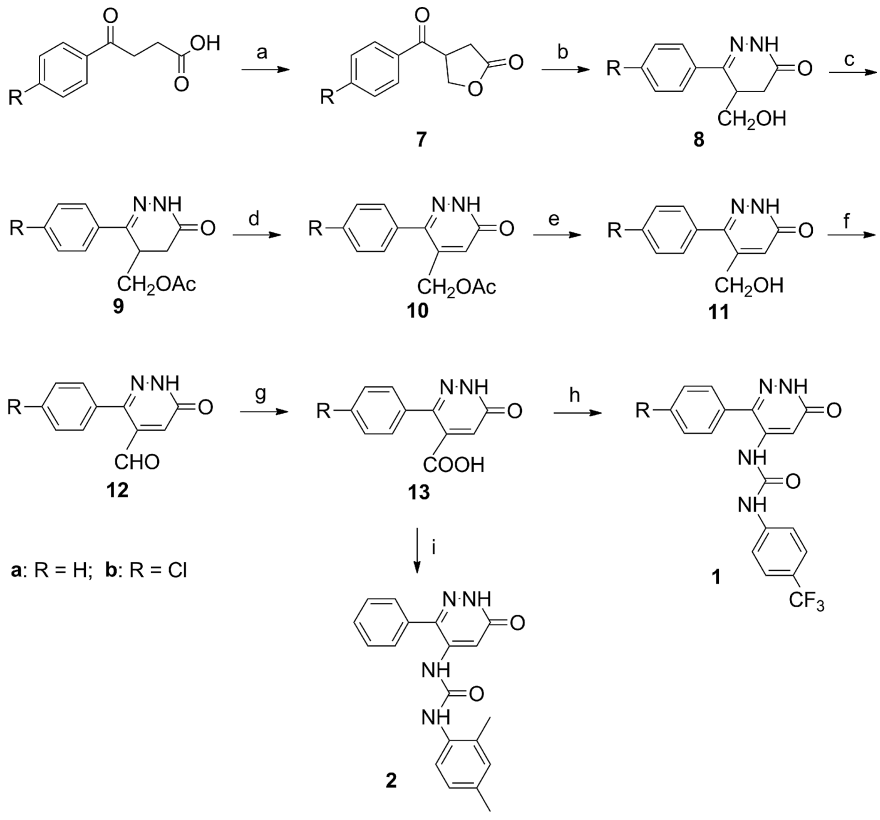

Scheme 1. Synthesis of compounds **1** and **2**. *Reagents and conditions:* (a) 1. HCHO (37%), NaOH; 2. HCl, room temp., 65% for **7b**; (b) NH_2NH_2, EtOH, reflux, 20% for **8b**; (c) Ac_2O, Py, room temp., 96% for **9b**; (d) MnO_2, $CHCl_3$, reflux, 20% for **10b**; (e) HCl (2 N), reflux, quantitative yield for **11b**; (f) MnO_2, THF, room temp., 55% for **12b**; (g) 1. $AgNO_3$, EtOH/H_2O 2. NaOH (10%), room temp., 70% for **13b**; (h) 1. DPPA, Et_3N, toluene, 80 °C; 2. 4-(trifluoromethyl)aniline, THF, reflux, 20% for **1a** and 10% for **1b**; (i) 1. DPPA, Et_3N, toluene, 80 °C; 2. 2,4-dimethylaniline, THF, reflux, 5%.

ues (τ_2 and τ_3) at the two *pseudo*-amide bonds, **1a** can show four different arrangements designated as *ZZ*, *ZE*, *EZ*, or *EE*.

The energy of the optimized conformations was recalculated by using a polarizable continuum solvent model[17] to highlight the effect of water on the population distribution of the conformers. In Table 1 the gas-phase and water-solvated energies of the minimum-energy conformers are reported, together with the corresponding percentage contributions to the overall population and the τ_1–τ_4 torsional angles. Figure 3 shows the three-dimensional plots of the most significant conformers. Only the members of the A family ($\tau_1 \approx 0$) are populated. In the gas phase, the preferred conformer is ***ZZ*_A**, which presents the *ZZ* arrangement at the two amide bonds (τ_2 = 176°, τ_3 = 178°) and accounts for about 93% of the overall population. Also conformers ***EZ*_A** (τ_2 = 19°, τ_3 = –179°) and ***ZE*_A** (τ_2 = 179°, τ_3 =

Table 1. Relative energy [kcal/mol], equilibrium percentages at 298 K, and τ_1–τ_4 torsional angles [°] of the B3LYP/6-311+G(d,p) located conformers of compound **1a**.

Conf.	E_{rel} vacuo	% vacuo	E_{rel} water	% water	τ_1	τ_2	τ_3	τ_4
***ZZ*_A**	0.00	92.7	0.0	99.1	–4	176	178	–3
***EZ*_A**	1.62	6.0	3.53	0.3	18	19	–179	4
***ZE*_A**	2.54	1.3	3.20	0.4	15	179	18	40
***EE*_A**	6.10	0.0	7.13	0.0	–2	42	34	18
***ZZ*_B**	4.72	0.0	3.72	0.2	122	178	175	–1
***EZ*_B**	4.64	0.0	5.73	0.0	120	1	176	–2
***ZE*_B**	7.49	0.0	7.11	0.0	121	–176	–2	57
***EE*_B**	9.49	0.0	10.17	0.0	143	–26	–34	–22

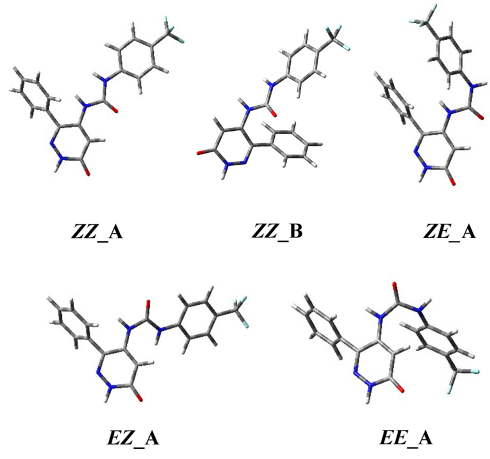

Figure 3. 3D plots of the most significant conformations of **1a**.

18°) present a not negligible population percentage, even if they are less stable than ***ZZ*_A** by 1.62 (6.0%) and 2.54 kcal/mol (1.3%), respectively. The relative energy of conformer ***EE*_A** (τ_2 = 42°, τ_3 = 34°) is much higher (6.10 kcal/mol) so that it gives no contribution to the overall population. It should be noted that the preference for conformer ***ZZ*_A** is almost complete in water and its population percentage exceeds 99%, contrary to reference compound **I** that showed, at the same level of calculations,[10] a small preference for a conformation of the ***ZZ*_B** type more stable by only 0.84 kcal/mol than its ***ZZ*_A** conformer.

Biological Evaluation

The STAT3 inhibitory activity of **1** and **2** was evaluated by means of a modified dual-luciferase assay[18] in human colorectal carcinoma cells HCT-116, characterized by uncontrolled expression of STAT3. After 24 h, inhibition percentages at 10 μM concentration of compounds **1a**, **1b**, and **2** were 26, 24, and 17%, respectively, whereas at 50 μM these values slightly increased to 33, 35, and 26%, respectively. Although the activity is approximately halved with respect to compound **I**[10] (70% at 10 μM and 75% at 50 μM), they still display moderate capability to interfere with the STAT3 pathway. Therefore, to investigate if these compounds are able to bind the STAT3 SH2 domain, an AlphaScreen-based assay was undertaken.[19] However, no significant results were obtained and the inhibition percentage was determined to be lower than ±20% at 30 μM.

Conclusions

In this article, we describe the design, synthesis and biological properties of new potential STAT3 inhibitors **1a**, **1b**, and **2** together with the modeling of **1a**. These compounds are characterized by a pyridazinone ring that replaces the 1,2,5-oxadiazole of reference compound **I**, a known agent for prevention and treatment of cancer.[9] The previous computational study carried out by us on **I** showed, for the urea, the *ZZ* conformation to be favored in water.[10] Styryl analogue **II**, which shows a significant drop in activity, prefers, both in vacuo and in water, the bent *EZ* geometry, which is stabilized by the formation of an intramolecular H-bond between an ureido NH hydrogen and the N2 oxadiazole. The modeling study on new pyridazinone **1a** revealed, both in vacuo and in water, an almost complete preference for the desired extended *ZZ* geometry. However, once tested with a dual-luciferase assay for their inhibition of the STAT3 signaling pathway, all compounds showed only modest activity. Furthermore, the AlphaScreen-based assay did not reveal any interaction with the STAT3 SH2 domain. These outcomes seem to indicate that neither the 1,2,5-oxadiazole ring, present in compound **II**, nor the extended *ZZ* arrangement, present in the new derivatives, alone is sufficient to confer significant activity against STAT3 and that they probably act in a synergistic way in compound **I**. It should also be noted that the N2 atom of the 1,2,5-oxadiazole ring might play two opposite roles. On one hand, it could favor the bent *EZ* ureido arrangement, which would be detrimental for activity, and on the other hand, it could play a specific role in the binding pocket of the SH2 domain by anchoring the ligand to the Arg609 residue, as shown by previous docking studies.[20]

Experimental Section

Materials and Methods: Reagents were purchased from commercial suppliers and used as received. Commercial plates on aluminum-backed Silica Gel 60 plates (0.2 mm, Merck) were used for analytical TLC to follow the course of the reaction. Silica gel 60 (Merck 40–63 μM) was used for flash chromatography to purify intermediates and final compounds. The purity of final compounds was determined by HPLC analysis and was ≥ 95%. Melting points were determined in open capillary tubes with a Buchi Melting Point 510. ^{1}H NMR spectra were acquired at ambient temperature with a 300 MHz Oxford-Varian instrument. Chemical shifts are expressed in ppm from tetramethylsilane resonance in the indicated solvent (TMS: δ = 0.0 ppm). Derivatives **3a**–**13a** were synthesized according to literature methods.[13–15] The structures of all compounds are consistent with their analytical and spectroscopic data.

Synthetic Procedures

β-(4-Chlorobenzoyl)-γ-butyrolactone (7b): Formaldehyde (37%, 3.08 mmol) was added to a stirred solution of 3-benzoyl-4-chloropropionic acid (2.81 mmol) and NaOH (0.5 N, 3.1 mmol; molar ratio of **6b**/CH_2O/NaOH = 1.0:1.1:1.1). After 1 h at room temperature, the mixture was acidified with concentrated hydrochloric acid (0.30 mL) and stirred for an additional 12 h. The mixture was extracted with ethyl acetate (3× 5 mL) and the combined organic layers were washed with NaOH (1 N, 5 mL), dried with anhydrous Na_2SO_4, and concentrated in vacuo. The crude mixture was purified by flash chromatography (eluent: dichloromethane/ethyl acetate, 97:3) to give **7b** (65% yield). ^{1}H NMR ($CDCl_3$): δ = 2.80 (m, 1 H, CH), 2.98 (m, 1 H, CH), 4.35 (m, 1 H, CH), 4.46 (m, 1 H, CH), 4.62 (m, 1 H, CH), 7.50 (m, 2 H, ArH), 7.88 (m, 2 H, ArH) ppm.

6-(4-Chlorophenyl)-5-(hydroxymethyl)-4,5-dihydro-3(2*H*)-pyridazinone (8b): Hydrazine monohydrate (0.78 mmol) was added to a solution of β-(4-chlorobenzoyl)-γ-butyrolactone (**7b**, 0.26 mmol) in ethanol (2 mL), and the mixture was heated to reflux for 1.5 h. The solvent was then removed in vacuo and the residue was extracted with ethyl acetate (5× 3 mL). The organic layer was dried with anhydrous Na_2SO_4, and concentrated in vacuo. Compound **8b** was obtained upon purification by flash column chromatography (eluent: dichloromethane/methanol, 95:5; 20% yield). ^{1}H NMR ($CDCl_3$): δ = 2.70 (m, 2 H, CH_2), 3.57 (m, 2 H, CH_2), 3.72 (m, 1 H, CH), 7.55 (m, 2 H, ArH), 7.86 (m, 2 H, ArH), 10.07 (s, 1 H, NH) ppm.

6-(4-Chlorophenyl)-5-(hydroxymethyl)-4,5-dihydro-3(2*H*)-pyridazinone Acetate (9b): Acetic anhydride (0.48 mmol) was added to a solution of 6-(4-chlorophenyl)-5-(hydroxymethyl)-4,5-dihydro-3(2*H*)-pyridazinone (**8b**, 0.25 mmol) in pyridine (2 mL), and the mixture was stirred at room temp. for 4 h. The pyridine was then removed under reduced pressure and the residue was extracted with ethyl acetate (5× 3 mL). The organic layer was dried with anhydrous Na_2SO_4, evaporated, and the crude mixture was purified by flash chromatography (eluent: cyclohexane/ethyl acetate, 3:7) to give **9b** (96% yield). ^{1}H NMR ($CDCl_3$): δ = 2.0 (m, 3 H, CH_3), 2.75 (m, 2 H, CH_2), 3.60 (m, 1 H, CH), 4.04 (m, 1 H, CH), 4.31

(m, 1 H, CH), 7.38 (m, 2 H, ArH), 7.75 (m, 2 H, ArH), 9.10 (s, 1 H, NH) ppm.

6-(4-Chlorophenyl)-5-(hydroxymethyl)-3(2*H*)-pyridazinone Acetate (10b): A mixture of 6-(4-chlorophenyl)-5-(hydroxymethyl)-4,5-dihydro-3(2*H*)-pyridazinone acetate (**9b**, 0.20 mmol) and activated manganese dioxide (2.1 mmol) in dry dichloromethane (2 mL) was heated to reflux for 24 h. After cooling, the oxidant was removed by filtration through Celite and the manganese dioxide was washed with dichloromethane. The filtrate was concentrated and the residue purified by flash chromatography (eluent: dichloromethane/ethyl acetate, 8:2; 20% yield). ^{1}H NMR ($CDCl_3$): δ = 2.13 (m, 3 H, CH_3), 4.88 (m, 2 H, CH_2), 7.05 (s, 1 H, CH), 7.35 (m, 2 H, ArH), 7.45 (m, 2 H, ArH), 10.8 (s, 1 H, NH) ppm.

6-(4-Chlorophenyl)-5-(hydroxymethyl)-3(2*H*)-pyridazinones (11b): A solution of 6-(4-chlorophenyl)-5-(hydroxymethyl)-3(2*H*)-pyridazinone acetate (**10b**, 0.20 mmol) in ethanol (3 mL) was treated with HCl (2 N, 1.5 mL) and the mixture was heated to reflux for 4 h. After cooling, the solvent was removed in vacuo and the residue extracted with ethyl acetate (4 × 3 mL). The organic layer was dried with anhydrous Na_2SO_4 and concentrated in vacuo to give **11b** in quantitative yield. ^{1}H NMR (CD_3COCD_3): δ = 2.85–3.05 (br. s, 1 H, OH), 4.45 (s, 2 H, CH_2), 7.20 (s, 1 H, CH), 7.50 (m, 4 H, ArH) ppm.

6-(4-Chlorophenyl)-5-formyl-3(2*H*)-pyridazinone (12b): A solution of 6-(4-chlorophenyl)-5-(hydroxymethyl)-3(2*H*)-pyridazinone (**11b**, 0.25 mmol) in dry tetrahydrofuran (THF; 2 mL) was stirred with activated manganese dioxide (2.5 mmol) for 48 h at room temp. The suspension was filtered through Celite and the manganese dioxide was washed with THF. The filtrate was concentrated and the residue purified by flash chromatography (eluent: dichloromethane/methanol, 95:5) to give **12b** (55% yield). ^{1}H NMR ($CDCl_3$): δ = 7.33 (s, 1 H, CH), 7.43 (m, 4 H, ArH), 9.91 (s, 1 H, CHO) ppm.

6-(4-Chlorophenyl)-5-carboxy-3(2*H*)-pyridazinone (13b): A solution of 6-(4-chlorophenyl)-5-formyl-3(2*H*)-pyridazinone (**12b**, 0.25 mmol) and silver nitrate (1.25 mmol) in ethanol (0.5 mL) and water (0.6 mL) was stirred rapidly under a nitrogen atmosphere. A NaOH (10%) solution was added until the reaction mixture reached pH 12. The resulting black suspension was stirred at room temperature for 15 h and then filtered. The filtrate was concentrated under reduced pressure, then acidified with HCl (6 N), extracted with diethyl ether (3 × 2 mL), dried with anhydrous Na_2SO_4, and concentrated in vacuo. The obtained crude mixture was purified by flash chromatography (eluent: dichloromethane/methanol, 9:1) to **13b** (70% yield). ^{1}H NMR ($CDCl_3$): δ = 6.20–6.82 (br. s, 1 H, COOH), 6.70 (s, 1 H, CH), 7.40 (d, 2 H, ArH), 7.60 (d, 2 H, ArH) 11.0 (s, 1 H, NH) ppm.

General Procedure A for the Synthesis of Compounds 1a and 1b: Diphenylphosphoryl azide (DPPA; 0.36 mmol) was added to a suspension of carboxylic acid (**13**, 0.23 mmol) in dry toluene (8 mL) and dry THF (8 mL) under a nitrogen atmosphere. Triethylamine (3.6 mmol) was dropped into the mixture that was stirred at room temperature for 30 min. The solution was heated at 80 °C for 2 h and then the appropriate substituted aniline (0.29 mmol) in THF (3 mL) was added together with triethylamine (3.6 mmol). After stirring at 80 °C overnight, the mixture was diluted with water (10 mL) and extracted with ethyl acetate (3 × 10 mL). The organic phase was washed with HCl (1 M, 1 × 10 mL), dried with anhydrous Na_2SO_4, and concentrated in vacuo to give the final products.

1-(6-Oxo-3-phenyl-1,6-dihydropyridazin-4yl)-3-(4-trifluoromethyl)-phenylurea (1a): General procedure A was followed to prepare final product **1a**, which was obtained as a white solid after purification by flash column chromatography (eluent: dichloromethane/methanol, 95:5; 20% yield), m.p. 154–156 °C. ^{1}H NMR (CD_3OD): δ = 7.55 (m, 9 H, ArH), 7.85 (s, 1 H, CH) ppm. HRMS (ESI): calcd. for $C_{18}H_{13}N_4O_2F_3Na$ [M + 1] 397.08828; found 397.08940.

1-[3(4-Chlorophenyl)-6-oxo-1,6-dihydropyridazin-4-yl]-3-(4-trifluoromethyl)phenylurea (1b): General procedure A was followed for the synthesis of compound **1b**, which was obtained as a pale yellow solid after purification by flash column chromatography (eluent: dichloromethane/methanol, 95:5; 10% yield), m.p. 161–162 °C. ^{1}H NMR (CD_3OD): δ = 7.59 (m, 8 H, ArH), 7.83 (s, 1 H, CH) ppm. HRMS (ESI): calcd. for $C_{18}H_{12}N_4O_2F_3ClNa$ [M + 1] 431.0431; found 431.05017.

1-(6-Oxo-3-phenyl-1,6-dihydropyridazin-4yl)-3-[2,4-(dimethyl)-phenyl]urea (2): General procedure A was followed for the synthesis of compound **2**, which was obtained as a white oil after purification by flash column chromatography (eluent: dichloromethane/methanol, 95:5; 5% yield). ^{1}H NMR (CD_3OD): δ = 2.11 (s, 3 H, CH_3), 2.26 (s, 3 H, CH_3), 6.95 (m, 2 H, ArH), 7.22 (s, 1 H, ArH), 7.50 (m, 5 H, ArH) ppm. HRMS (ESI): calcd. for $C_{19}H_{18}N_4O_2$ [M + 1] 335.15025; found 335.14865.

Dual Luciferase Assay

Cell Culture: Human colon cancer cell line (HCT-116) was obtained from American Type Culture Collection and it was maintained in McCoy's 5A (Gibco/BRL). The culture medium was supplemented with heat-inactivated fetal bovine serum (10%; Gibco/BRL). Cell cultures were maintained at 37 °C under a humidified atmosphere of CO_2 (5%) in an incubator.

Transient Transfection and Dual-luciferase Assays:[18] HCT-116 cells were seeded at a density of 10×10^5 cells in a 100 mm^2 culture plate. The cells were co-transfected with pSTAT3-TA-Luc (27 μg/plate) and internal control plasmid pRL-TK (9 μg/plate) that contained *Renilla* luciferase gene. All plasmids used in this experiment were purchased from Promega. Transfection was carried out by using TransFectin (Bio-Rad) in accordance with the manufacturer's protocol. Then, 5 h after transfection, the cells were trypsinized and seeded onto sterilized black bottom 96-well plates at a density of 1×10^4 cells per well. The following day, cells were treated with test compounds and incubated for 24 h. Firefly and *Renilla* luciferase activities were measured by using dual-light reporter gene assay kit (Promega) with a Wallac Victor2 (Perkin–Elmer, Inc., Wellesley, MA). *Renilla* luciferase activity was determined to calibrate transfection efficiency and cytotoxicity of chemicals. Relative STAT3 activity was calculated by dividing the firefly luciferase activity with *Renilla* luciferase activity in each transfection experiment. The values of STAT3 inhibitory activity were the mean results of three experiments and the maximum deviation from the mean was less than 10%.

AlphaScreen-Based Assay: AlphaScreen is a bead-based nonradioactive assay system to detect biomolecular interactions in microtiter plate format. Binding of biological partners brings donor and acceptor beads into close proximity and as a result, a fluorescent signal between 520 and 620 nm is produced. The AlphaScreen-based assays[19] were performed in a final reaction volume of 25 μL of the assay buffer that contained 4-(2-hydroxyethyl)-1-piperazine-ethanesulfonic acid–NaOH (10 mM, pH 7.4), NaCl (50 mM), ethylenediaminetetraacetic acid, (1 mM, pH 8.0), NP-40 (0.1%), and bovine serum albumin (10 ng/μL) in a 96-well microtiter plate at 25 °C. The phospho-Tyr (pTyr) peptide probes used in this study were 5-carboxyfluorescein (FITC)-GpYLPQTV for STAT3, FITC-GpYDKPHVL for STAT1, and FITC-PSpYVNVQN for Grb2.

each SH2-containing protein (75 nM) was incubated with the test compound for 15 min. Each protein sample was then incubated for 90 min with its corresponding FITC-pTyr peptide (50 nM), and mixed with streptavidin-coated donor beads and *anti*-FITC acceptor beads simultaneously before detection at 570 nm with a EnVisonXcite (PerkinElmer).

Modeling Studies: The modeling study of compound **1a** was performed with the Gaussian09[21] program package through optimizations in the gas-phase at the B3LYP level with the 6-311+G(d,p) basis set.[16] Vibrational frequencies were computed at the same level of theory to define the optimized structures as minima. Solvent effects (water) were considered by single-point calculations, at the same level as above, on the gas-phase optimized geometries, by using a self-consistent reaction field method, based on the polarizable continuum model.[17]

Acknowledgments

The authors acknowledge the financial support of the Universities of Milan and Pavia and the Italian Ministero dell'Università e della Ricerca (MIUR) (funds PRIN 2010-11). B. M. K. was supported by the KRIBB Research Initiative Program and the Bio-Synergy Research Project (2012M3A9C404877).

[1] J. E. Darnell Jr., *Science* **1997**, *277*, 1630–1635.
[2] H. Yu, R. Jove, *Nat. Rev. Cancer* **2004**, *4*, 97–105.
[3] R. Buettner, L. B. Mora, R. Jove, *Clin. Cancer Res.* **2002**, *8*, 945–954.
[4] J. E. Darnell Jr., *Nat. Med.* **2005**, *11*, 595–596.
[5] D.-S. Shin, H.-N. Kim, K. D. Shin, Y. J. Yoon, S.-J. Kim, D. C. Hanand, B.-M. Kwon, *Cancer Res.* **2009**, *69*, 193–202.
[6] T. Bowman, M. A. Broome, D. Sinibaldi, W. Wharton, W. J. Pledger, J. M. Sedivy, R. Irby, T. Yeatman, S. A. Courtneidge, R. Jove, *Proc. Natl. Acad. Sci. USA* **2001**, *98*, 7319–7324.
[7] J. Turkson, D. Ryan, J. S. Kim, Y. Zhang, Z. Chen, E. Haura, A. Laudano, S. Sebti, A. D. Hamilton, R. Jove, *J. Biol. Chem.* **2001**, *276*, 45443–45455.
[8] D. Masciocchi, A. Gelain, S. Villa, F. Meneghetti, D. Barlocco, *Future Med. Chem.* **2011**, *3*, 367–397.
[9] B.-M. Kwon, D. C. Han, K.-H. Son, D.-S. Shin, J. Lee, US 20080051442.
[10] D. S. Shin, D. Masciocchi, A. Gelain, S. Villa, D. Barlocco, F. Meneghetti, A. Pedretti, Y.-M. Han, D. C. Han, M. Y. Han, B.-M. Kwon, L. Legnani, L. Toma, *MedChemComm* **2010**, *1*, 156–164.
[11] S. Villa, D. Masciocchi, A. Gelain, F. Meneghetti, *Chem. Biodiversity* **2012**, *9*, 1240–1253.
[12] D. Masciocchi, A. Gelain, F. Meneghetti, A. Pedretti, G. Celentano, D. Barlocco, L. Legnani, L. Toma, B.-M. Kwon, A. Asai, S. Villa, *MedChemComm* **2013**, *4*, 1181–1188.
[13] E. Sotelo, E. Ravina, I. Estevez, *J. Heterocycl. Chem.* **1999**, *36*, 985–990.
[14] R. Laguna, B. Rodriguez-Linares, E. Cano, I. Estevez, E. Ravina, E. Sotelo, *Chem. Pharm. Bull.* **1997**, *45*, 1151–1155.
[15] G. Cignarella, G. Grella, M. M. Curzu, *Synthesis* **1980**, *10*, 825–828.
[16] a) C. Lee, W. Yang, R. G. Parr, *Phys. Rev. B* **1988**, *37*, 785–789; b) A. D. Becke, *J. Chem. Phys.* **1993**, *98*, 5648–5652.
[17] a) E. Cances, B. Mennucci, J. Tomasi, *J. Chem. Phys.* **1997**, *107*, 3032–3042; b) M. Cossi, V. Barone, R. Cammi, J. Tomasi, *Chem. Phys. Lett.* **1996**, *255*, 327–335; c) V. Barone, M. Cossi, J. Tomasi, *J. Comput. Chem.* **1998**, *19*, 404.
[18] B. A. Sherf, S. L. Navarro, R. R. Hannah, K. V. Wood, *Promega Notes Mag.* **1996**, *57*, 2–8.
[19] Y. Uehara, M. Mochizuki, K. Matsuno, T. Haino, A. Asai, *Biochem. Biophys. Res. Commun.* **2009**, *380*, 627–631.
[20] D. Masciocchi, S. Villa, F. Meneghetti, A. Pedretti, L. Legnani, L. Toma, B.-M. Kwon, S. Nakano, A. Asai, A. Gelain, *MedChemComm* **2012**, *3*, 592–599.
[21] M. J. Frisch, G. W. Trucks, H. B. Schlegel, G. E. Scuseria, M. A. Robb, J. R. Cheeseman, G. Scalmani, V. Barone, B. Mennucci, G. A. Petersson, H. Nakatsuji, M. Caricato, X. Li, H. P. Hratchian, A. F. Izmaylov, J. Bloino, G. Zheng, J. L. Sonnenberg, M. Hada, M. Ehara, K. Toyota, R. Fukuda, J. Hasegawa, M. Ishida, T. Nakajima, Y. Honda, O. Kitao, H. Nakai, T. Vreven, J. A. Montgomery Jr., J. E. Peralta, F. Ogliaro, M. Bearpark, J. J. Heyd, E. Brothers, K. N. Kudin, V. N. Staroverov, R. Kobayashi, J. Normand, K. Raghavachari, A. Rendell, J. C. Burant, S. S. Iyengar, J. Tomasi, M. Cossi, N. Rega, J. M. Millam, M. Klene, J. E. Knox, J. B. Cross, V. Bakken, C. Adamo, J. Jaramillo, R. Gomperts, R. E. Stratmann, O. Yazyev, A. J. Austin, R. Cammi, C. Pomelli, J. W. Ochterski, R. L. Martin, K. Morokuma, V. G. Zakrzewski, G. A. Voth, P. Salvador, J. J. Dannenberg, S. Dapprich, A. D. Daniels, O. Farkas, J. B. Foresman, J. V. Ortiz, J. Cioslowski, D. J. Fox, *Gaussian 09*, revision A.02, Gaussian, Inc., Wallingford CT, **2009**.

Received: May 11, 2015
Published Online: June 30, 2015

